Bulletin of the Seismological Society of America, Vol. 99, No. 2B, pp. 1190–1198, May 2009, doi: 10.1785/0120080171

Ring Laser Measurements of Ground Rotations for Seismology

by K. U. Schreiber, J. N. Hautmann, A. Velikoseltsev, J. Wassermann, H. Igel, J. Otero, F. Vernon, and J.-P. R. Wells

Abstract Since the discovery of the wave nature of light, optical interferometry has assumed an important place in high precision metrology. This is mostly due to the inherent high sensor resolution for operational wavelengths in the vicinity of several hundred nanometers. In this context, interferometers in the Michelson configuration are most prominently used in gravitational wave antennas, such as the large projects VIRGO, LIGO, TAMA, and GEO600. In the Sagnac configuration they are used for high resolution rotation monitoring such as the precise observation of Earth rotation. Modern large-scale ring lasers reach a sensitivity for the measurement of rotation of 1 prad/sec (with approximately 1 hr of averaging). Because of the comparatively short wavelengths employed, optical interferometers are extremely sensitive to small mechanical perturbations of the entire apparatus. These can be caused by deformations, thermal or mechanical stress, and instabilities in the alignment of the optical components at the level of about $\lambda/100$. Ring lasers suitable for geophysical applications require a sensor resolution in the range of 10^{-8} rad/sec and below. This demands a scale factor of the instrument that is only achievable with mechanical dimensions of the interferometer on the order of about 1 m^2 or larger. At the same time the necessary mechanical rigidity of the entire instrument has to be on the order of 5 nm. Currently, this has only been achieved with monolithic ring lasers made from blocks of Zerodur and installed in a temperature stabilized underground environment. However if long-term sensor stability is not required, compromises can be made and, in particular for studies of regional seismic events, it becomes feasible to build a heterolithic rotation sensor in a simpler and much cheaper way. Here, we report the design and first results from the GEOsensor, which has been specifically constructed for studies in rotational seismology. The sensor is operated at the Piñon Flat Seismological Observatory in Southern California.

Introduction

Currently there are two types of measurements that are routinely used to monitor global and regional seismic-wave fields. Standard inertial seismometers measure three components of translational ground displacement (velocity and acceleration) and form the basis for monitoring seismic activity and ground motion. The second type aims at measuring the deformation of the Earth (strains). It has been noted for decades (Aki and Richards, 1980, 2002) that there is a third type of measurement that is needed in seismology and geodesy in order to fully describe the motion at a given point, namely the measurement of ground rotation. The three components of seismically-induced rotation have been extremely difficult to measure, primarily because previous devices did not provide the required sensitivity to observe rotations in a wide frequency band and distance range (the two horizontal components, equal to tilt at the free surface, are generally recorded at low frequencies, but are polluted by additional inertial effects). Indeed, Aki and Richards (2002) note on page 608 that "seismology still awaits a suitable instrument for making such measurements." Furthermore, the angular motion amplitudes were expected to be small even in the vicinity of faults (Bouchon and Aki, 1982), whereas there is growing evidence that these amplitudes have been underestimated (e.g., Castellani and Zembaty, 1996).

Following the pioneering observations with ring laser rotation sensors in Christchurch, New Zealand (McLeod *et al.*, 1998; Pancha *et al.*, 2000), and other work (Takeo, 1998; Takeo and Ito, 1997), a purpose-built ring laser for the observation of the Earth's rotation rate located at Wettzell, Germany (Schreiber *et al.*, 2006), was adapted to the sampling rate requirements in seismology. This allows the observation of earthquake-induced rotational ground motions over a wide magnitude and epicentral distance range (Igel *et al.*, 2005: Cochard *et al.*, 2006; Igel *et al.*, 2007).

Analysis of these observations in combination with collocated recordings by a standard broadband seismometer showed the possibility of extracting additional seismograms on subsurface structure compared to translational measurements alone (e.g., Suryanto *et al.*, 2006; Ferreira and Igel, 2008; Fichtner and Igel, 2008), otherwise accessible only with seismic array measurements. These studies and earlier considerations motivated the development of a ring laser (denoted as the GEOsensor) specifically designed for seismological purposes given an observatory infrastructure. A prototype of this rotational sensor was installed at the Piñon Flat Seismological Observatory in 2005.

The aim of this article is to describe the technical details of this rotation sensor and to discuss issues related to the installation and operation. Furthermore, examples of earthquake-induced rotation measurements from the GEOsensor are presented. The comparison with collocated translational measurements confirms the previously established consistency with plane-wave theory and, thus, the validity of the rotation measurements (Igel *et al.*, 2005).

Sensor Design and Properties

The high sensitivity for rotations of large ring lasers along with their insusceptibility to linear translations makes the application of these instruments very attractive for studies of rotational signals from seismic events. The required range of angular velocities to be measured is expected to be 10^{-14} rad/sec $\leq \mathbf{\Omega}_s \leq 1$ rad/sec and the required frequency bandwidth for the seismic waves is in the range of 3 mHz $\leq f_s \leq 10$ Hz (Schreiber, Velikoseltsev, Stedman, *et al.*, 2004). Three such devices mounted in orthogonal orientations will eventually provide the quantitative detection of rotations from shear, Love, and Rayleigh waves; thus, providing the missing quantities for a complete 6 degrees of freedom measurement system. Ring lasers are active interferometers, where two laser beams are circulating around a polygonal closed cavity in opposite directions (Aronowitz, 1971). If the whole apparatus is rotating with respect to inertial space, one obtains a frequency splitting of the two counter-propagating waves, which is proportional to the rate of rotation. The observed beat frequency δf is

$$\delta f = \frac{4A}{\lambda P}\mathbf{n} \cdot \mathbf{\Omega}, \tag{1}$$

where A is the area, P is the perimeter enclosed by the beam path, and λ is the optical wavelength of the laser oscillation. $\mathbf{\Omega}$ is the angular velocity at which the instrument is turning and $\mathbf{n}$ is the normal vector to the laser beam plane. The resolution of a ring laser gyroscope increases as the size of the cavity increases. When first installed, the GEOsensor reached a sensor resolution of $\delta\varphi = 10^{-10}$ rad/sec$/\sqrt{\text{Hz}}$. This outstanding sensitivity is suitable for the detection of both teleseismic waves and near source signals. Typical seismic events require high sensor stability for up to one hour of continuous data acquisition. This requirement is significantly reduced from the long-term stability necessary for the measurement of Earth rotation variations (Schreiber *et al.* 2003; Schreiber, Velikoseltsev, Rothacher, *et al.*, 2004), where the sensor drift has to be negligible over a timespan of many months.

A ring laser for seismology must be capable of accurately recording seismic rotation rates, while keeping the scaling factor (the quotient in equation 1) constant. At the same time the whole sensor must be relocatable, be cost effective, and allow for a relatively simple installation. Given the fact that a ring laser is a highly sensitive optical interferometer, all these requirements are essentially conflicting design goals. In order to achieve a workable concept, the interferometer is assembled from several individual components. Four mechanically stable corner boxes with individually integrated alignment elements are bolted to a thick concrete platform, which provides the necessary rigid geometric reference. In order to obtain a stable interferogram of the two laser beams, the cavity length has to remain constant to within a small fraction of the optical wavelength. Therefore, ring lasers have to be placed in a temperature controlled underground laboratory (see discussion in the Operational Issues section).

The frequency band of interest for a rotational sensor in seismology covers about 5 orders of magnitude, while the corresponding sensitivity for the measurement of rotations should cover 14 orders of magnitude, the range between strong motion during a local earthquake on one side and the weak signals of a remote earthquake more than 10,000 km away on the other side. However, if we exclude the strong-motion domain and very weak signals from the immediate regime of interest, we obtain a viable measurement range for a prototype sensor of approximately 10^{-12} rad/sec $\leq \mathbf{\Omega}_s \leq 10^{-4}$ rad/sec, which still extends over 8 orders of magnitude. Most of this range is covered by large ring laser gyroscopes, such as the GEOsensor. Figure 1 gives an impression of the actual ring laser design. The laser cavity has the shape of a square. The four turning mirrors are each located at the center of adjustable stainless steel containers inside the solid corner boxes. As shown in the right-hand side of the figure, a folded lever system allows the alignment of each mirror mount to be within ± 10 sec of arc. This high level of alignment is required to ensure lasing from an op-

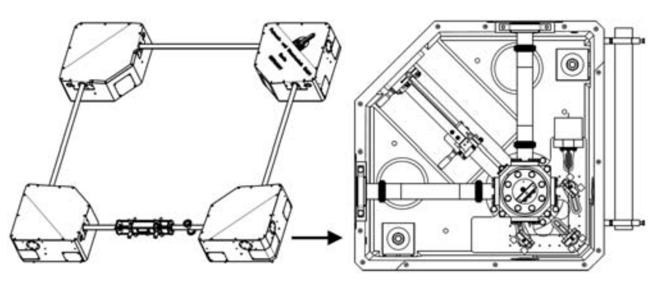

Figure 1. Construction diagram of the GEOsensor ring laser.

tically stable cavity. The steel containers in turn are linked together with stainless steel tubes, forming an evacuated enclosure for the laser beams. In the middle of one side, the connecting steel tube is reduced to a glass capillary of 4 mm inner diameter and a length of 10 cm, which is required for gain medium excitation. When operated, the ring laser cavity is first evacuated and then filled with a mixture of helium and neon, reaching a total gas pressure of approximately 6 hPa. The following three important considerations are unique for the GEOsensor design:

- The ring laser interferometer is constructed from several mechanically rigid components. Therefore, it can be transported in reasonably sized containers without compromising the stability.
- It requires a stable concrete platform at the location of deployment. Such a pad is simple to specify and can be prepared independently of the actual GEOsensor deployment.
- The actual size of the ring laser is not limited by the design. The instrument can be customized according to the available space at the host observatory. Different GEOsensor realizations may, therefore, have different sizes and, consequently, different instrumental resolution. The length of the current instrument is 1.6 m on a side, which provides a total area of 2.56 m^2.

In order to operate the GEOsensor, the cavity must be evacuated, baked to reduce outgassing, and filled with helium and neon at a mixing ratio of 30:1. This procedure requires a turbo molecular pump system and a manifold with a supply of highly graded ^4He,^{20}Ne, and ^{22}Ne. The pump system is not required during the operation of the GEOsensor. It is only necessary for the preparation of the sensor operation and is used three to four times during a year in order to renew the laser gas. Laser excitation itself is achieved via a radio frequency generator (Stedman, 1997) matched to a symmetrical parallel high-impedance antenna at the gain tube. A feedback loop maintains a constant laser beam intensity inside the ring laser and ensures monomode operation. When the ring laser is operated, it detects the beat note caused by the Earth's rotation.

The required high-mechanical stiffness for the interferometer at the Piñon Flat Seismological Observatory is obtained from a 30 cm thick concrete slab, which makes up most of the laboratory floor. Figure 2 shows the construction of the rotation sensor. In the event of an earthquake the entire slab rotates rigidly without deformation and the Sagnac interferometer determines the rotation rate of the slab. The sensitivity of the ring laser is determined by the scale factor $(4A/\lambda P)$ of the instrument as defined according to equation (1). Technically, the GEOsensor represents a continuous-wave gas laser with an extremely high-quality factor of $Q = \omega\tau = 2\pi \times 474$ THz $\times$ 0.001 sec $\approx 10^{12}$, with τ being the ring down time of the laser cavity and ω being the frequency of the laser beam. The high value of Q and the cavity dimensions determine the extraordinary sensor resolution.

Because the ring laser is rigidly tied to the ground at the Piñon Flat Seismological Observatory, the output signal is rate biased by the Earth's rotation, which generates a constant beat note (or Sagnac frequency). This rate bias offsets the earthquake signals from zero, that is, away from the highly nonlinear lock-in region of the ring laser (Wilkinson, 1987). Because **n** is the normal vector on the ring laser beam plane and $\mathbf{\Omega}$ points along the rotational axis having a magnitude given by $2\pi/86,164$ sec (1 revolution per siderial day), only a fraction of the Earth's rotation is contained in the measurement. At a latitude of 33.5° N, corresponding to the location of the Piñon Flat Seismological Observatory in Southern California, the ring laser beat frequency δf becomes 107.2 Hz for a horizontally oriented instrument. Seismically-induced rotation signals show up as a frequency modulation of this otherwise constant rate bias (Schreiber *et al.*, 2005). In practice, the concrete slab of the GEOsensor installation appears to be slightly tilted towards south, so that the actual observed Sagnac frequency is around 102 Hz.

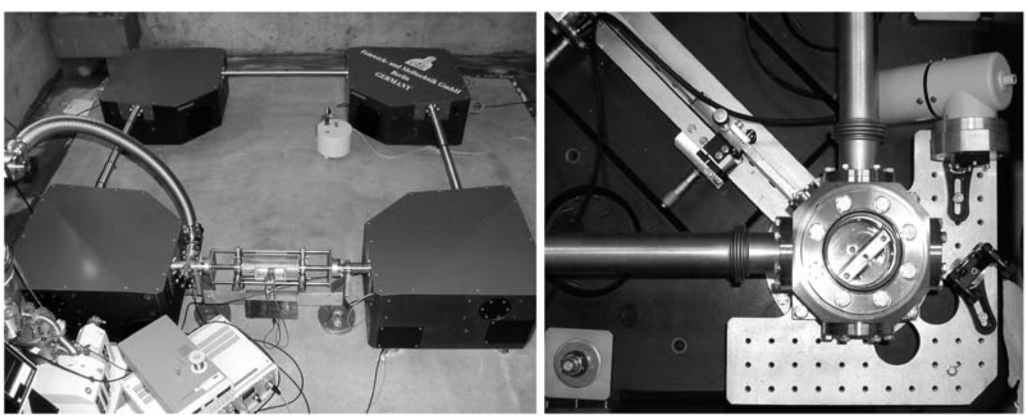

Figure 2. Complete ring laser mechanics mounted on a rigid concrete slab in an underground laboratory (left-hand panel). The lever system with one of the mirrors inside the vacuum enclosure is used to align the laser cavity under ultra-high vacuum conditions (right-hand panel).

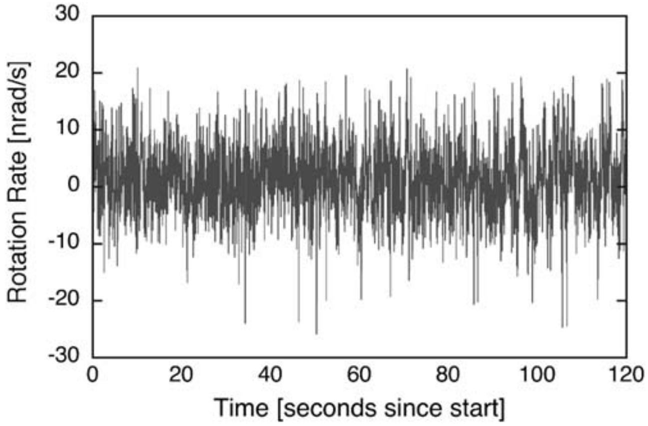

Figure 3. Time series of the instantaneous measured rate of rotation of the GEOsensor taken at the Piñon Flat Seismological Observatory.

Sensor Performance and Operational Issues

Sensor Performance

Once the interferogram of the two counter-propagating laser beams is established one can determine the variation of this beat note at a rate of 20 Hz. With an integration time of 50 msec and the current performance of the frequency estimator, the sensor resolution is as high as 20 nrad/sec under stable operating conditions as shown in Figure 3. This is enough to establish the rotation rate caused by teleseismic signals as well as a local seismic event. Figure 4 shows an example for a small local tremor generating rotation rates of approximately 150 nrad/sec at maximum. Further examples of teleseismic earthquakes are presented and discussed in the Observations section. While the obtained sensor resolution is within 1 order of magnitude of the theoretical limit caused by shot noise (Schreiber *et al.*, 2008), there is still some room for improvement.

In order to extract the variations of the Sagnac frequency from the Earth-induced rate bias, a demodulation technique is employed. A voltage controlled oscillator (VCO) is slaved

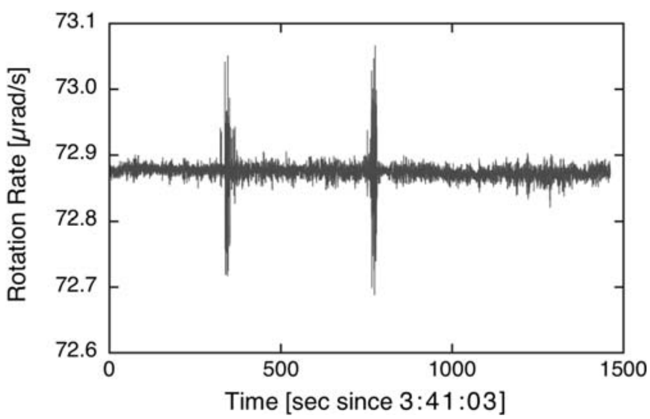

Figure 4. Example of two small local tremors measured in Piñon Flat. The observed rotation rates are up to 150 nrad/sec.

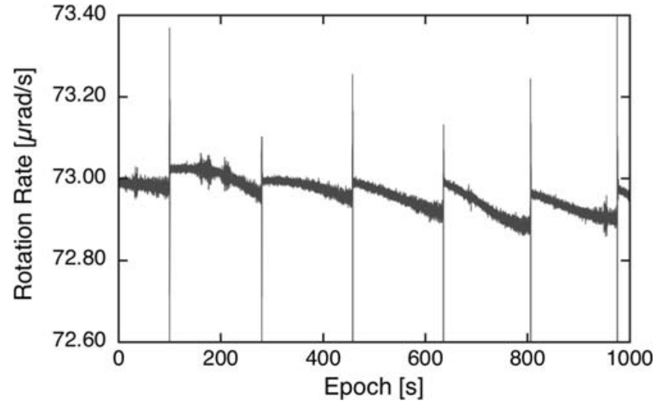

Figure 5. Sudden longitudinal mode changes cause disruptions in the interferogram. Normally these effects occur quite rapidly. Ground motion between such mode changes is retrievable.

to the output frequency of the interferometer via a phase-locked loop (PLL). While the feedback voltage of the PLL serves as a voltage proportional to the rate of change of frequency, the sensor is still limited in resolution by how tightly the VCO can be locked to the input Sagnac frequency. A tight lock corresponds to a small capture range, which limits the dynamic range of the entire sensor. A sloppy lock on the other hand gives a wide dynamic range, but restricts the lower limit of the sensor's sensitivity. The current setup is a compromise, which excludes a very wide dynamic range and also reduces the available sensor sensitivity. However, there is a capacity to tune the instrument as appropriate for either of the two limits of operation.

Operational Issues

The GEOsensor is located in an underground laboratory in order to keep temperature fluctuations to a minimum. Despite all precautions, the interferometer experiences temperature changes of several degrees even within one day. In response to that, both the concrete foundation as well as

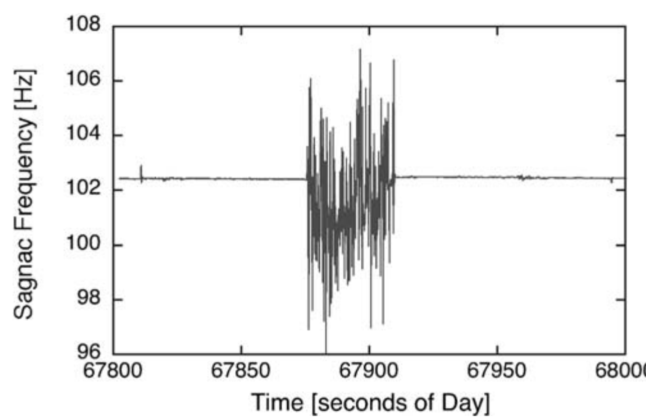

Figure 6. Sudden longitudinal mode changes, within the laser, can result in the simultaneous presence of two modes with different longitudinal indices. For as long as this state of operation persists, there is no detectable audio beat frequency.

Table 1
List of Earthquakes Discussed

Date (yyyy/mm/dd)	Time (hh:mm:ss UTC)	Latitude (°)	Longitude (°)	Magnitude	Region	Distance (°)	S/N* (Acceleration)	S/N* (Rotation)	Phase Velocity (m/sec)	Peak Correlation Coefficient
2006/04/20	23:25:20	167.08	60.95	7.6	Kamchatka	54.81	528	94	5197	0.95
2006/05/24	04:20:28	−115.27	32.44	5.4	Mexico	1.53	4313	590	4648	0.92
2007/05/20	09:40:43	32.97	−115.92	3.6	California	0.78	561	34	8670	0.96
2007/05/24	06:11:39	34.20	−117.38	3.9	California	0.97	14352	97	14512	0.98

*S/N stands for signal-to-noise ratio.

the laser cavity expand or shrink by several λ, giving rise to perturbations of the interferogram because of longitudinal mode index changes. The effect of such mode hops is shown in Figure 5. This complication was known in the design phase of the GEOsensor, but it was accepted because otherwise the construction would have become prohibitively expensive. Because local earthquakes are usually very short, they usually happen in the regime between data glitches caused by mode jumps. Therefore, it is possible to extract many of the earthquakes during postprocessing, as Figure 5 illustrates. While mode jumps in the case of large temperature gradients are frequent, they reduce to about one event per hour under normal operating conditions. Also visible is a slow drift in the observed Earth rotation rate, which is caused by dispersion effects in the laser gain medium. For teleseismic events, a substantial reduction of the mode jumps is desirable, because signals from remote earthquakes contain ground motion at much lower frequencies and, hence, longer duration. Another complication is the possibility that a mode change results in a situation where two modes with different longitudinal indices coexist in the ring laser cavity. This causes the Sagnac frequency at 102 Hz to disappear. The rotational signal would still be there, but it is shifted in frequency by one free spectral range (for the GEOsensor, 46.875 MHz) and, therefore, becomes inaccessible for the current detection electronics, as shown in Figure 6. An active perimeter control eventually will take care of these issues.

Observations

In 2006 and 2007 several earthquakes were recorded by the GEOsensor, located in California. In this study, the rota-

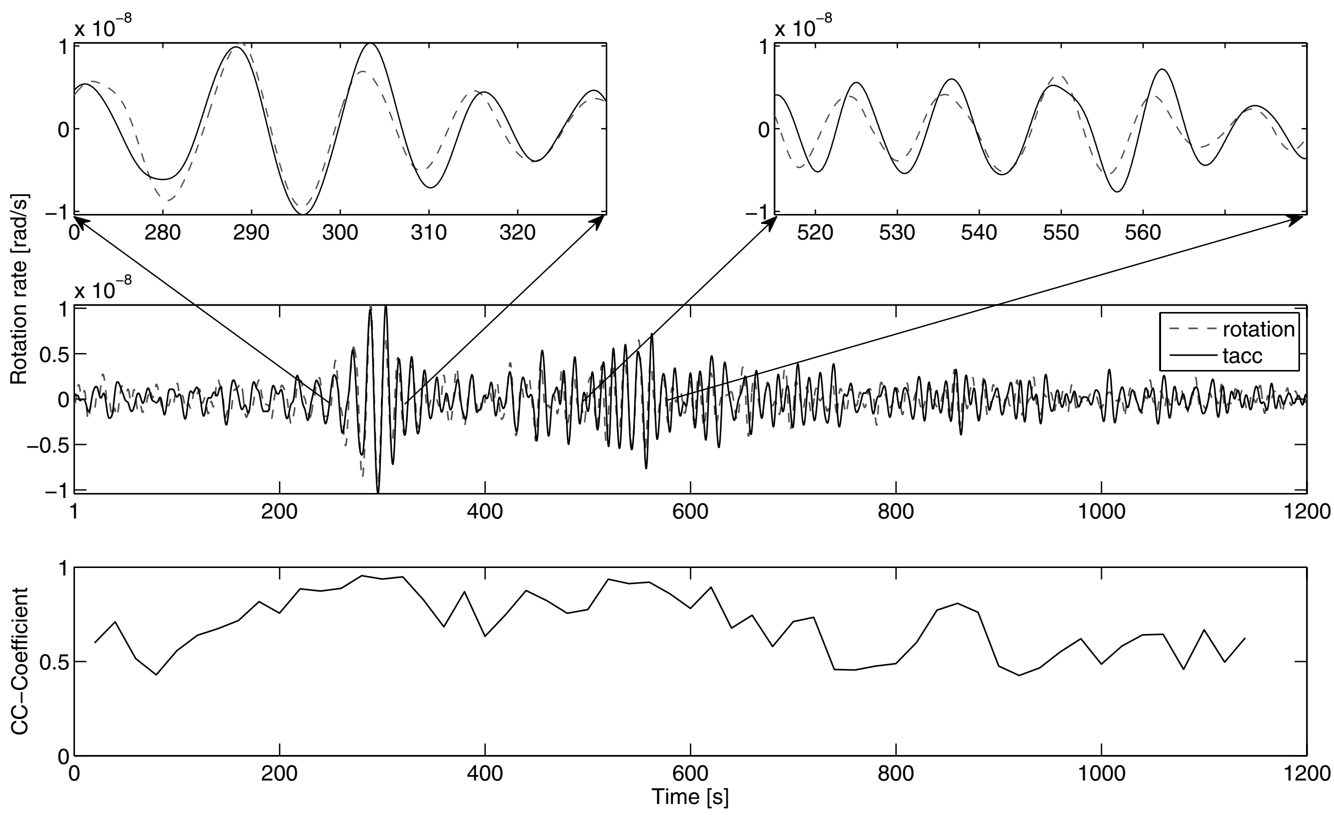

Figure 7. 20 April 2006 M 7.6 Kamchatka event: superposition of the vertical component of rotation rate (dashed curve) in rad/sec and transverse acceleration (solid curve, amplitude scaled to match) recorded by the GEOsensor, plus the corresponding maximum cross-correlation coefficients in a 20 sec sliding time window for a back azimuth of 324.5°.

tional and translational signals measured by the ring laser component of the GEOsensor and the collocated seismometer, a Lennartz LE-3D 20 s, are compared. Four events with diverse magnitudes and epicentral distances, and, therefore, varying frequency content, are chosen to show the quality of the recorded data. All observations are summarized in Table 1. To evaluate the observed data and the consistency with theory (e.g., Igel *et al.*, 2005), the vertical component of rotation rate $\vec{\Omega}_z$ is directly compared with the corresponding transverse acceleration $\vec{a}$ according to

$$\vec{\Omega}_z(x,t) = -\frac{\vec{a}(x,t)}{2c_p}, \tag{2}$$

with c_p as the horizontal phase velocity underneath the measurement point. Assuming plane-wave propagation and transverse polarization, the rotational and translational signals should match in waveform and the amplitude difference is two times the phase velocity.

In order to analyze the recorded data, each of the events is low-pass filtered and processed depending on the individual frequency content. The transverse acceleration is obtained by the differentiation of the transverse component of translation in time, with respect to the back-azimuth angle. The extent to which the phase between the signal obtained by the rotation sensor and the transverse acceleration agrees is quantified by the cross-correlation coefficient. This time dependent similarity is expressed by zero-lag cross-correlation coefficients with values between 0 and 1 (marking none or perfect agreement) as a function of time in a sliding time window.

In Figure 7, the superposition of rotation rate and transverse acceleration for the 20 April 2006 *M* 7.6 Kamchatka event is presented. The time window (middle panel) with a length of 1200 sec presents the obtained rotation rate (dashed curve) and transverse acceleration (solid curve) as a function of time. The two enlarged plots (top panels) emphasize the similarity in the waveform of the signals in two selected time windows. In the bottom panel the cross-correlation coefficient is presented as a function of time. The strong increase in correlation with the surface-wave arrival to a maximum coefficient of 0.95 is clearly visible. Noticeable is the high level of cross-correlation in the surface-wave section, around 0.8 before going back to 0.5 and below. According to equation (2), the estimated peak phase velocity is $c_p = 5197$ m/sec.

The rotational seismogram of a regional earthquake, the 24 May 2006 *M* 5.4 Mexico event, is shown in Figure 8, again compared to transverse acceleration. The sections of highest cross-correlation coefficients are enlarged

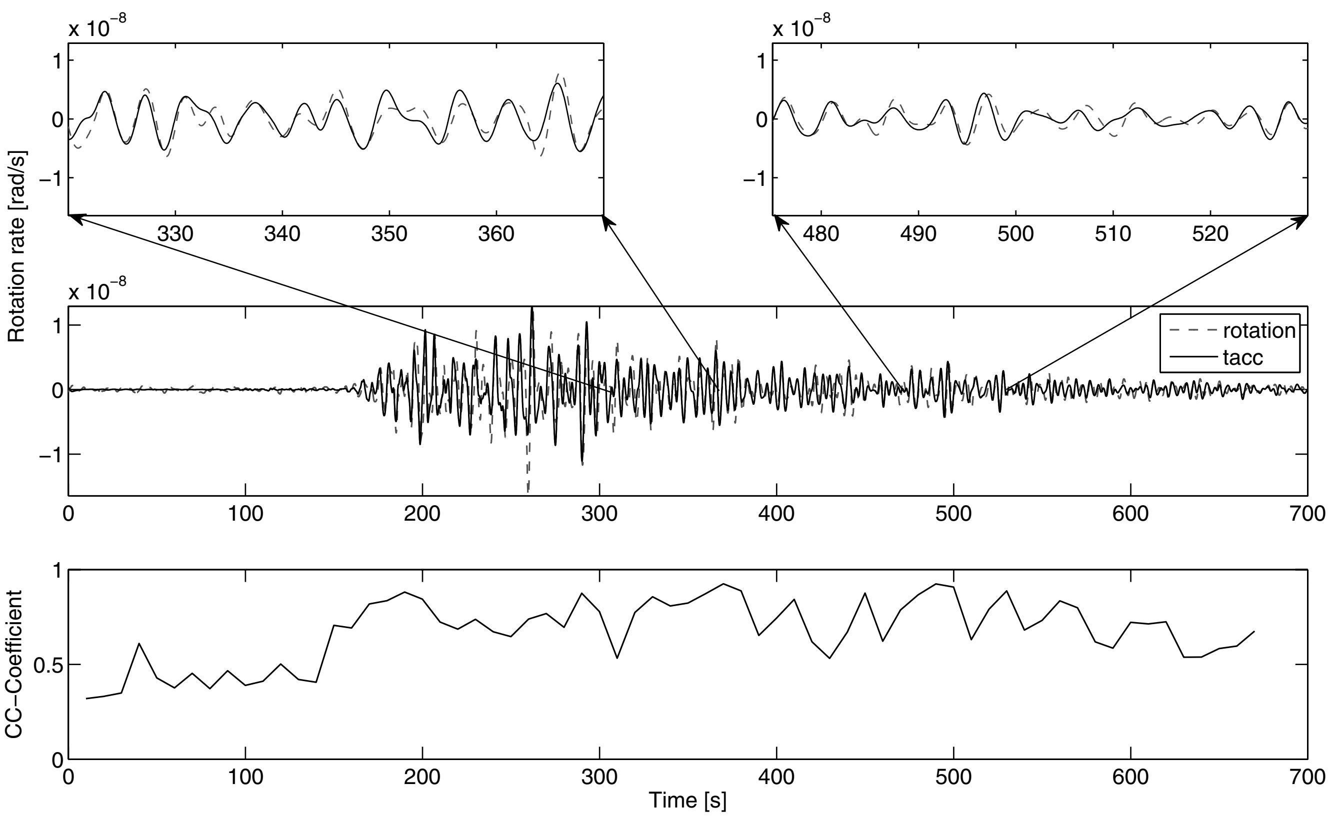

Figure 8. 24 May 2006 *M* 5.4 Mexico event: superposition of the vertical component of rotation rate (dashed curve) in rad/sec and transverse acceleration (solid curve, amplitude scaled to match) recorded by the GEOsensor, plus the corresponding maximum cross-correlation coefficients in a 20 sec sliding time window for a back azimuth of 139.2°.

(top panels). Before the Love-wave onset, a cross-correlation coefficient of less than 0.5 is obtained, which increases to high values during the entire event with a maximum coefficient of 0.92. The corresponding peak phase velocity amounts to $c_p = 4648$ m/sec. To demonstrate the GEOsensor's ability for obtaining the rotation rate from local events, two California earthquakes presented in Figures 9 and 10 were chosen. Both events are shallow, 4 and 12 km, respectively, and have a epicentral distance of less than 1°. Figure 9 shows the 20 May 2007 *M* 3.6 event and Figure 10 shows the 24 May 2007 *M* 3.9 event. A clearly visible good fit between rotation rate and transverse acceleration phases during the *S*-wave section is supported by a peak in cross-correlation coefficients for both superposition plots. The largest values reach 0.96 and 0.98, respectively.

The apparent mismatch in waveform following the *S*-wave section might be explained by a reduced validity of the plane-wave assumption for events with very low epicentral distances. The resulting maximum phase velocities are relatively high with values of $c_p = 8670$ m/sec and $c_p = 14,512$ m/sec. These high phase velocities are likely to be caused by the oblique incidence of the body-wave phases as observed before in other ring laser measurements (Igel *et al.*, 2005). The overall good agreement in waveform demonstrates the suitability of the GEOsensor for geoscientific studies over a wide range of source distances and magnitudes. The presented cross-correlation coefficients affirm expectations from theory, even though Figures 9 and 10 are suffering from the plane-wave assumption for small distances.

Discussion and Conclusions

Despite decades of high-quality broadband seismometry, there are still issues that are poorly understood. This relates, in particular, to the components of rotations around three orthogonal axes to which translational sensors are also sensitive. The two components of rotation around the horizontal axes are usually referred to as tilts (at the free surface). Tiltmeters are sensitive to horizontal accelerations and are, thus, not capable of providing a pure rotational signal. The advent of large ring lasers (originally designed for geodetic purposes) has led to the first accurate recordings of coseismic rotations primarily around the vertical axis (e.g., Pancha *et al.*, 2000; Igel *et al.*, 2005). These observations motivated the development of the GEOsensor, a ring laser sensor specifically designed for seismology, as reported here. Because of the short wavelength used in these optical interferometers, they are very sensitive to ambient variations such as temperature and pressure changes. The effects on the rotational mea-

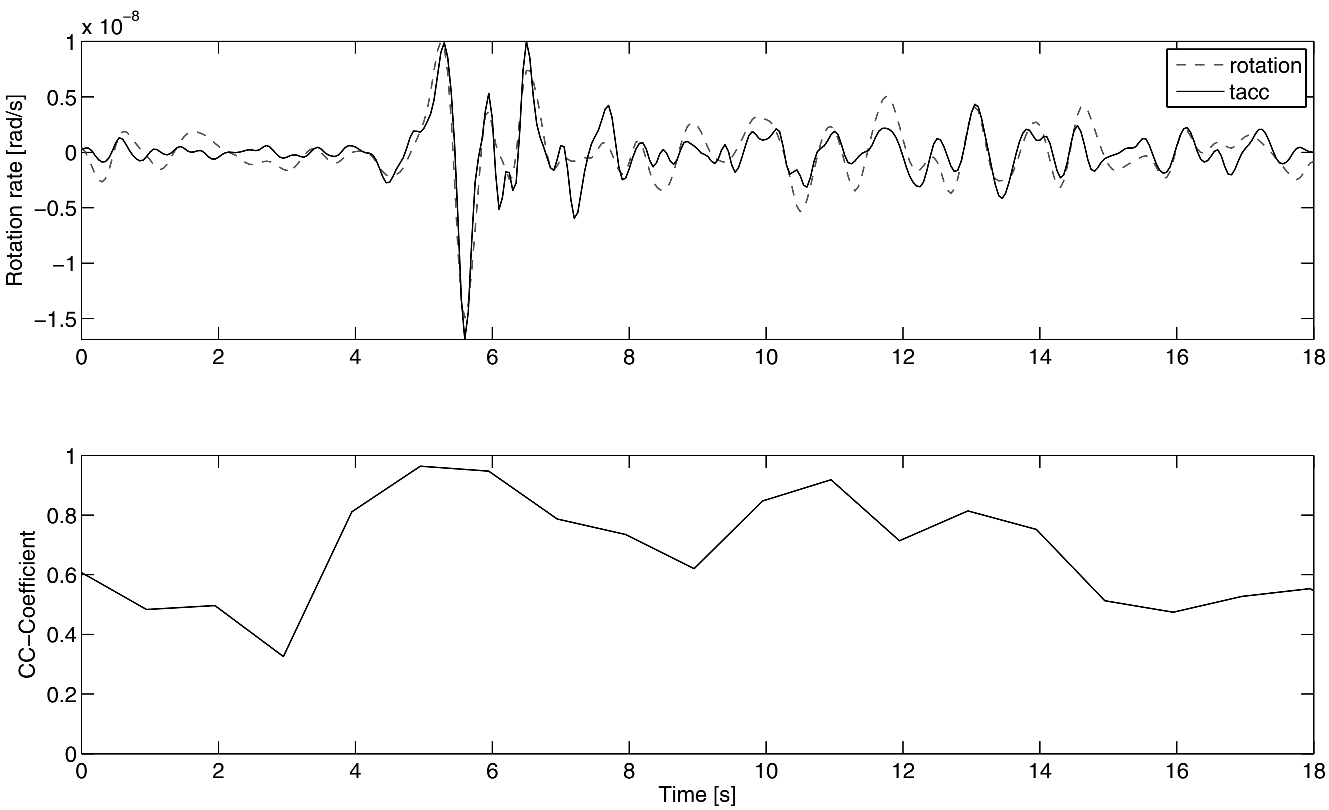

Figure 9. 20 May 2007 *M* 3.6 California event: superposition of the vertical component of rotation rate (dashed curve) in rad/sec and transverse acceleration (solid curve, amplitude scaled to match) recorded by the GEOsensor, plus the corresponding maximum cross-correlation coefficients in a 2 sec sliding time window for a back azimuth of 144.7°.

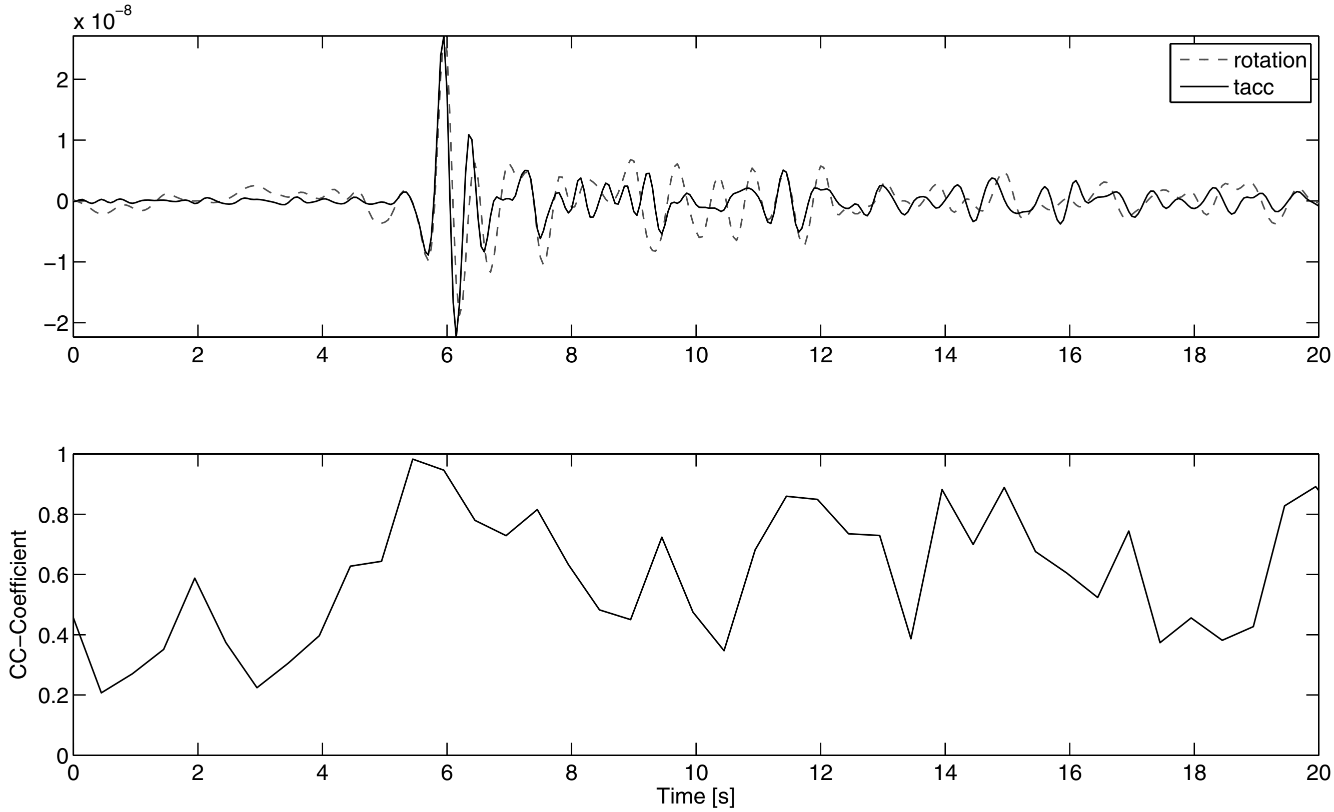

Figure 10. 24 May 2007 *M* 3.9 California event: superposition of the vertical component of rotation rate (dashed curve) in rad/sec and transverse acceleration (solid curve, amplitude scaled to match) recorded by the GEOsensor, plus the corresponding maximum cross-correlation coefficients in a 1 sec sliding time window for a back azimuth of 307.7°.

surements (e.g., longitudinal mode hops) are in large part due to temperature fluctuations at the Piñon Flat Seismological Observatory.

Nevertheless, a large set of data has been accumulated, demonstrating the consistent observation of rotational ground motions when compared to recordings of standard seismometers. This has been previously shown for the much more expensive monolithic ring laser system in Wettzell, Germany. While efforts are underway to understand the performance of alternative rotation sensors (Wassermann *et al.*, 2009) with a much smaller dynamic range, which might be applicable in the near field under certain limited circumstances, there still is a need to investigate the fundamental physics of observing complete ground motion. This has relevance for large-scale experiments like the gravitational wave detection (e.g., VIRGO and LIGO) where the quality of the observations strongly depends on decoupling the observing system from the ground motions in the 1 Hz regime. This is only possible if all components are known. In light of this, we propose to establish multicomponent seismic observatories (displacements, velocities or accelerations, and rotations, plus strain) combined with (i.e., surrounded by) a small-aperture broadband array, with which cross validation (e.g., Suryanto *et al.*, 2006; Wassermann *et al.*, 2009) is possible.

Data and Resources

All data used in this article were acquired by the authors on the GEOsensor at the Piñon Flat Seismological Observatory in Southern California.

Acknowledgments

This work was supported by the Bundesministerium für Bildung und Forschung (BMBF), Grant Number 03F0325 A-D under the Geotechnology Program and Deutsche Forschungsgemeinschaft Grant Number Ig16/8. H.I. acknowledges support through a Cecil-and-Ida Green Fellowship of the Scripps Institution of Oceanography, La Jolla.

References

Aki, K., and P. G. Richards (1980). *Quantitative Seismology*, First Ed., W. H. Freeman, New York.

Aki, K., and P. G. Richards (2002). *Quantitative Seismology*, Second Ed., University Science Books, Sausalito, California.

Aronowitz, F. (1971). *The Laser Gyro. Laser Applications*, M. Ross, (Editor), Vol. **1**, Academic, New York, 133–200.

Bouchon, M. B., and K. Aki (1982). Strain, tilt, and rotation associated with strong ground motion in the vicinity of earthquake faults, *Bull. Seismol. Soc. Am.* **72,** 1717–1738.

Castellani, A., and Z. Zembaty (1996). Comparison between earthquake spectra obtained by different experimental sources, *Eng. Struct.* **597,** 603–618.

Cochard, A., H. Igel, B. Schuberth, W. Suryanto, A. Velikoseltsev, K. U. Schreiber, J. Wassermann, F. Scherbaum, and D. Vollmer (2006). Rotational motions in seismology: theory, observation, simulation., in *Earthquake Source Asymmetry, Structural Media and Rotation Effects*, R. Teisseyre, M. Takeo, and E. Majewski (Editors), chap. 30, Springer, New York.

Ferreira, A. M. G., and H. Igel (2009). Rotational motions of seismic surface waves in a laterally heterogeneous Earth, *Bull. Seismol. Soc. Am.* **99,** no. 2B, 1429–1436.

Fichtner, A., and H. Igel (2009). Sensitivity densities for rotational ground-motion measurements, *Bull. Seismol. Soc. Am.* **99,** no. 2B, 1302–1314.

Igel, H., A. Cochard, J. Wassermann, A. Flaws, K. U. Schreiber, A. Velikoseltsev, and N. Pham Dinh (2007). Broad-band observations of earthquake-induced rotational ground motions, *Geophys. J. Int.* **168,** 182–196.

Igel, H., K. U. Schreiber, B. Schuberth, A. Flaws, A. Velikoseltsev, and A. Cochard (2005). Observation and modelling of rotational motions induced by distant large earthquakes: the *M* 8.1 Tokachi-oki earthquake September 25, 2003, *Geophys. Res. Lett.* **32,** L08309, doi 10.1029/2004GL022336.

McLeod, D. P., G. E. Stedman, T. H. Webb, and K. U. Schreiber (1998). Comparison of standard and ring laser rotational seismograms, *Bull. Seismol. Soc. Am.* **88,** 1495–1503.

Pancha, A., T. H. Webb, G. E. Stedman, D. P. McLeod, and K. U. Schreiber (2000). Ring laser detection of rotations from teleseismic waves., *Geophys. Res. Lett.* **27,** 3553–3556.

Schreiber, K. U., H. Igel, A. Velikoseltsev, A. Flaws, B. Schuberth, W. Drewitz, and F. Müller (2005). The GEOsensor project: rotations—a new observable for seismology, in *Observation of the Earth System from Space*, Springer, New York, 427–447.

Schreiber, K. U., G. E. Stedman, H. Igel, and A. Flaws (2006). Ring laser gyroscopes as rotation sensors for seismic wave studies, in *Earthquake Source Asymmetry, Structural Media and Rotation Effects*, R. Teisseyre, M. Takeo, and E. Majewski (Editors), chap. 29, Springer New York.

Schreiber, K. U., G. E. Stedman, and T. Klügel (2003). Earth tide and tilt detection by a ring laser gyroscope, *J. Geophys. Res.* **108,** no. B, 2132, doi 10.1029/2001JB000569.

Schreiber, K. U., A. Velikoseltsev, M. Rothacher, T. Klügel, G. E. Stedman, and D. L. Wiltshire (2004). Direct measurement of diurnal polar motion by ring laser gyroscopes., *J. Geophys. Res.* **109,** no. B6, B06405, doi 10.1029/2003JB002803.

Schreiber, K. U., A. Velikoseltsev, G. E. Stedman, R. B. Hurst, and T. Klügel (2004). Large ring laser gyros as high resolution sensors for applications in geoscience, *Proc. of the 11th International Conf. on Integrated Navigation Systems*, St. Petersburg, 24–26 May 2004, 326–331.

Schreiber, K. U., J.-P. R. Wells, and G. E. Stedman (2008). Noise processes in large ring lasers, *J. Gen. Relativ. Gravity* **40,** no 5, 935–943, doi 10.1007/s10714-007-0584-2.

Stedman, G. E. (1997). Ring laser tests of fundamental physics and geophysics, *Rep. Prog. Phys.* **60,** 615–688.

Suryanto, W., H. Igel, J. Wassermann, A. Cochard, B. Schuberth, D. Vollmer, F. Scherbaum, K. U. Schreiber, and A. Velikoseltsev (2006). First comparison of array-derived rotational ground motions with direct ring laser measurements, *Bull. Seismol. Soc. Am.* **96,** 2059–2071.

Takeo, M. (1998). Ground rotational motions recorded in near-source region of earthquakes, *Geophys. Res. Lett.* **25,** 789–792.

Takeo, M., and H. M. Ito (1997). What can be learned from rotational motions excited by earthquakes?, *Geophys. J. Int.* **129,** 319–329.

Wassermann, J., S. Lehndorfer, H. Igel, and U. Schreiber (2009). Performance test of a commercial rotational motions sensor, *Bull. Seismol. Soc. Am.*, **99,** no. 2B, 1449–1456.

Wilkinson, J. R. (1987). Ring lasers, *Prog. Quantum Electron.* **11,** 1–103.

Technische Universitaet Muenchen
Forschungseinrichtung Satellitengeodaesie Fundamentalstation Wettzell
93444 Bad Kötzting, Germany
schreiber@fs.wettzell.de
(K.U.S., A.V.)

Department of Earth and Environmental Sciences
Ludwig-Maximilians-University Munich
Theresienstrasse 41
D-80333 Munich, Germany
(J.N.H., J.W., H.I.)

Cecil H. and Ida M. Green Institute of Geophysics and Planetary Physics
Scripps Institution of Oceanography
University of California, San Diego
9500 Gilman Drive
La Jolla, California 92093-0225
(J.O., F.V.)

Department of Physics and Astronomy
University of Canterbury
Private Bag 4800
Christchurch 8020, New Zealand
(J.-P.R.W.)

Manuscript received 5 July 2008